
Supplementary Online Content

Cheng W, Rolls ET, Ruan H, Feng J. Functional connectivities in the brain that mediate the association between depressive problems and sleep quality. *JAMA Psychiatry*. Published online July 25, 2018. doi:10.1001/jamapsychiatry.2018.1941

eMethods. Materials and Methods

eFigure 1. The correlation between the PSQI total score and the other available sleep measures in the HCP dataset, based on the sample of 1017 individuals.

eFigure 2. The Shen atlas areas with functional connectivities related to sleep quality.

eFigure 3. Brain areas with functional connectivities related to both the sleep quality (PSQI) and the ASR DSM Depressive Problems scores from the HCP analysis.

eFigure 4. Brain areas with functional connectivities related to the ASR DSM Depressive Problems scores from the HCP analysis.

eFigure 5. Mediation analysis.

eTable 1. The anatomical regions defined in each hemisphere.

eTable 2. Functional connectivities related to the ASR DSM Depressive Problems scores from the HCP analysis using 1017 participants.

eTable 3. Functional connectivities correlated with the ASR DSM Depressive Problems scores from the HCP analysis based on the 92 participants who had at some time been diagnosed with depression.

eTable 4. The results of the mediation analysis performed for the 39 individual links that were correlated with sleep quality and the Depressive Problems score.

eTable 5. The demographic characteristics of participants of the Biobank dataset.

eReferences.

This supplementary material has been provided by the authors to give readers additional information about their work.

© 2018 American Medical Association. All rights reserved.

eMethods. Materials and Methods

Primary dataset from the Human Connectome Project

The dataset used for this investigation was selected from the Mar 2017 public data release from the Human Connectome Project (HCP, N = 1200), WU-Minn Consortium. Our sample includes 1017 subjects (ages 22–35 years, 546 females) scanned on a 3-T Siemens connectome-Skyra scanner. Two resting state fMRI acquisitions on different days were used. The four resting-state runs of approximately 15 minutes each were acquired in separate sessions on two different days, with eyes open with relaxed fixation on a projected bright cross-hair on a dark background. The WU-Minn HCP Consortium obtained full informed consent from all participants, and research procedures and ethical guidelines were followed in accordance with the Institutional Review Boards (IRB). The demographic characteristics of participants are summarized in Table 1. More details of subjects, the collection and preprocessing of the data are provided at the HCP website (<http://www.humanconnectome.org/>). Briefly, data pre-processing was carried out using FSL (FMRIB Software Library), FreeSurfer, and the Connectome Workbench software. All the data preprocessing procedures were performed by the human connectome project (HCP) as described in ¹. The data preprocessing included correction for spatial and gradient distortions and head motion, intensity normalization and bias field removal, registration to the T1 weighted structural image, transformation to 2 mm Montreal Neurological Institute (MNI) space, and the FIX artefact removal procedure ^{2,3}. Finally, the head motion parameters are regressed out and structured artefacts are removed by ICA+FIX processing (Independent Component Analysis followed by FMRIB's ICA-based X-noiseifier ^{4,5}). The data preprocessing pipeline developed by FMRIB (Oxford University Centre for Functional MRI of the Brain) used here has been widely used in resting state fMRI studies ^{2,6-8}.

The first 20 volumes were discarded to suppress equilibration effects and participants without the full 1200 time points in four resting-state runs were also removed from the following analysis. The resulting time courses were used for the construction and analysis of the brain network.

Cross-validation dataset: the UK Biobank dataset

The initial release of UK Biobank imaging data was used for cross-validation and consisted of 9850 subjects (ages 46–78 years, 5155 females) scanned on a single standard Siemens Skyra 3T scanner. After quality controls and removing some participants without behavioral data, 8718 participants remained in this study. The UK Biobank received ethical approval from the research ethics committee (REC reference 11/NW/0382). The present analyses were conducted under UK Biobank application number 1954. Written informed consent was obtained from each subject. The demographic characteristics of participants are summarized in Table S5. The details of the image acquisition are provided at the UK Biobank website in the form of a protocol (<http://biobank.ctsu.ox.ac.uk/crystal/refer.cgi?id=2367>). All the quality checking and data preprocessing procedures were conducted by the UK Biobank and the details of the preprocessing are available on the UK Biobank website (<http://biobank.ctsu.ox.ac.uk/crystal/refer.cgi?id=1977>) and elsewhere ⁹. Briefly, the following pre-processing was applied: motion correction; grand-mean intensity normalization of the entire 4D dataset by a single multiplicative factor; high-pass temporal filtering (Gaussian-weighted least-squares straight line fitting, with sigma=50.0s); EPI unwarping; gradient distortion correction unwarping. Finally, the head motion parameters are regressed out and structured artefacts are removed by ICA+FIX processing (Independent Component Analysis followed by FMRIB's ICA-based X-noiseifier ^{4,5}). Basically, the parameters and data preprocessing procedures are very consistent in both datasets which make the UK Biobank dataset useful for cross-validating the findings described here based on the HCP dataset.

Construction of the whole-brain functional network

After preprocessing, the whole brain (gray matter) was parcellated into 250 regions of interest (ROI) using the Shen atlas ¹⁰ which has also been validated in resting state fMRI

© 2018 American Medical Association. All rights reserved.

studies^{11,12}, with further details below. Then the time series were extracted in each ROI by averaging the signals of all voxels within that region. The names of the ROIs are listed in Supplementary Table 1 and the modified atlas is also provided on the website: <http://www.dcs.warwick.ac.uk/~feng/>. (This is a standard parcellation scheme, which provides a usable number of different divisions for statistical purposes when differences between regions are being investigated, and includes a useful parcellation of the orbitofrontal cortex.). The Pearson cross-correlations between all pairs of regional BOLD signals were calculated for each subject followed by z-transformation to improve normality, and the whole-brain functional connectivity network (250×250 region-based network with 31,125 edges) was constructed. Finally, the mean functional connectivity across two scans (each scan containing left to right and right to left phase encoding directions) was used for the following analysis to provide a more reliable estimation of functional connectivity.

To address the problem of multiple comparisons, the network-based statistic (NBS)¹³ which is a well-validated method for brain network association analysis and has previously been used widely in neuroimaging studies¹³⁻¹⁶ was used to identify and ascribe significance to any connected sub-networks evident in the set of significantly altered links found in the poor sleep quality group (see Supplementary Material). The NBS has been described in detail previously¹³. In brief, a primary threshold for each link-based *r* value was set to the stringent criterion of $p < 0.001$ ¹³, corresponding in this study to an absolute $r > 0.103$, and used to identify a set of supra-threshold links. Any connected components in these supra-threshold links and their size (the number of links) were then determined. Finally, a FWE-corrected *p*-value for each component was calculated using the null distribution of maximal connected components which was derived empirically using a nonparametric permutation approach (10,000 permutations).

The rationale for use of the Shen atlas

The parcellation of the brain used in this investigation was the Shen atlas¹⁰, which was found to be useful in this investigation because it has more areas than the AAL2 (automated anatomical labelling version 2) atlas¹⁷. Since the parcellation of the orbitofrontal cortex in the Shen atlas is less useful than the AAL2 atlas, we modified the Shen atlas so that it includes the AAL2 parcellation produced by Rolls et al¹⁷ of the medial orbitofrontal cortex areas (OFC_med, OFC_ant, OFC_post, Rectus, and OLF) and lateral orbitofrontal cortex areas (OFC_lat and Frontal_Inf_Orb2). Because the Shen atlas areas do not have individual names, we show the mapping of Shen atlas areas to AAL2 atlas areas in Table S1, and use these names when referring to particular brain areas and their functional connectivity. The AAL2 atlas is available with MRICron (<http://people.cas.sc.edu/rorden/mricron/>).

The parcellation maps provided as part of the HCP⁸ utilize independent component analysis (ICA) to parcellate the brain and have been used in many studies. However, for the following reasons, we chose to use the Shen atlas rather than HCP atlas.

1. The parcellation maps provided by the HCP group are based on an ICA method which is a data-driven method. Therefore, different datasets would provide different parcellation maps. However, in the current study, we used another independent dataset (the UK Biobank) to cross-validate the findings driven by the HCP dataset. If we used the HCP atlas in our analysis, it would be difficult to perform this very valuable cross-validation analysis.

2. One of the important findings is that many significant results are related to the orbitofrontal cortex, and this brain area is not well defined in the HCP atlas.

3. The Shen atlas¹⁰ was also created based on resting state fMRI data and has been validated in resting state fMRI studies^{11,12} which are consistent with the current work.

Cross-validation using the UK Biobank dataset

We used another separate large dataset (the UK Biobank dataset) which included 8718 participants to test whether the above findings are robust and generalize to another population. Given there is no PSQI score in the Biobank dataset, we selected another important measure of sleep, the amount of sleep (sleep duration), which is available for both datasets to test

© 2018 American Medical Association. All rights reserved.

whether the FCs identified in these two datasets are similar. Specifically, linear regression analysis was used to test whether the associations between the amount of sleep and functional connectivity are similar in these independent datasets. This approach is supported by the fact that a correlation of -0.51 was found between the PSQI total score and the sleep duration in a large study involving 1039 participants¹⁸.

The average sleep duration (for a 24 hour day in the last 4 weeks) which is high negatively correlated with the PSQI score ($r = -0.574$, $p < 1.0 \times 10^{-80}$, Fig. S5), was used to test whether the FCs identified in these two datasets are similar. The association patterns between FCs and sleep duration are very similar in both the HCP dataset and the Biobank dataset (Fig. 3A). Fig. 3B shows that there is a high positive correlation ($r=0.524$, $p < 1.0 \times 10^{-30}$) between the r values for the correlation between the functional connectivity links for the whole brain and the sleep duration based on the HCP and Biobank datasets. Further, a Fisher's test also confirmed the correlation ($p < 10^{-10}$). Then a permutation test showed that the 162 significant links identified in Fig. 1B were also negatively correlated with sleep duration in the Biobank dataset ($p = 2.0 \times 10^{-4}$). Further, we found that 89 out of the 162 significant links were also significant after FDR correction ($p < 0.05$) in the Biobank dataset. This cross-validation analysis thus provides evidence that the sleep-related links described here can be confirmed with an independent dataset.

Mediation Analysis

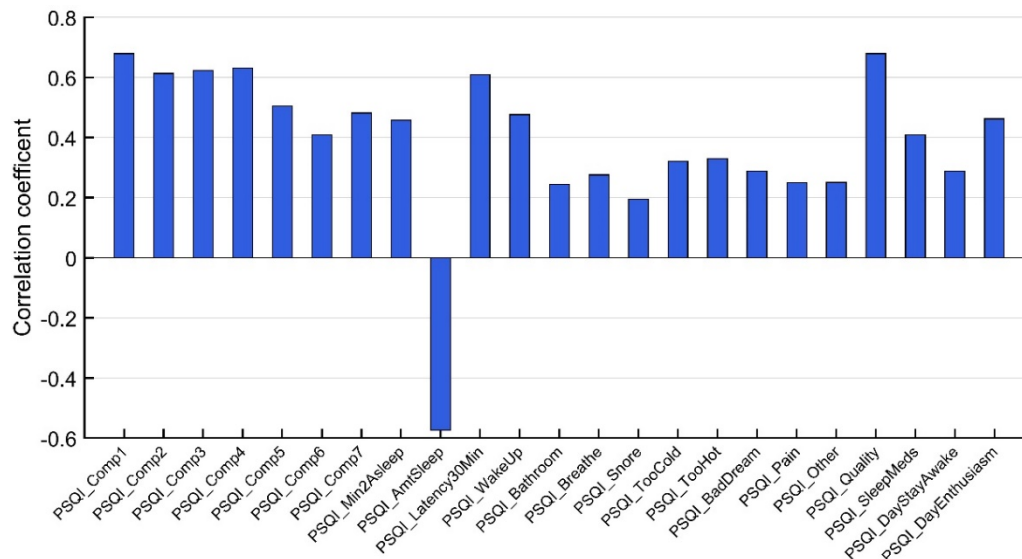
Given that the strengths of the functional connectivities were significantly associated with the sleep quality measure (PSQI) score and depressive score, we assessed whether the functional connectivities significantly mediated¹⁹ the association between the depressive problems score and the PSQI score. The mediation analysis¹⁹ was performed using the Mediation Toolbox developed by Tor Wager (<https://github.com/canlab/MediationToolbox>), with a 10,000 bias-corrected bootstrap sample for significance testing. The independent (predictor) and dependent (predicted) variables were the depressive score and the sleep quality measure, respectively. The proposed mediator was the strength of functional connectivities associated with sleep quality. Mediation analyses controlled for the 14 confounding variables described in the main paper.

The mean strength of the 39 significant functional connectivities shown in Fig. 1D involved in both poor sleep quality and depressive problems significantly mediated the relationship between the PSQI score and depressive problems score (Fig. 2D, path AB) (4.8% of the total effect size, $\beta = 0.0139$; $p = 2.1 \times 10^{-5}$; 95% CI, 0.01 to 0.03). This provides evidence that the 39 functional connectivity links may account for this proportion of the relation of poor sleep quality on depressive problems.

Further, we also performed the same analysis on each individual functional connectivity link. We found that all 39 links significantly mediated the relationship between the PSQI sleep quality and the depressive problem score (using FDR correction, $p < 0.05$, Table S4). In the reverse direction, only 2 links significantly mediated effects of sleep quality on depressive problems with FDR correction. Further, the mediating effects of the 39 functional connectivities of the effects of the sleep quality on the depressive problems had much lower significance (3.4% of the total effect size, $\beta = 0.016$, $p = 0.0095$, Fig. S4) than for the effect in the opposite direction described above. In other words, the increases of the 39 functional connectivities shown in Fig. 1D mediated the effect of depressive problems on sleep quality, and the effect was weaker in the opposite direction.

We note that the functional connectivities only partially mediated the association between the depressive score and the PSQI score, with 4.8% of the total effect being mediated by these functional connectivities (Fig. 2D). Factors that may contribute to the remaining 95.2% include higher firing rates of neurons in brain areas related to depression on brain areas involved in sleep.

Figure 1. The correlation between the PSQI total score and the other available sleep measures in the HCP dataset, based on the sample of 1017 individuals. All measures are highly correlated with PSQI total score ($p < 1.0 \times 10^{-10}$). 19 out the 23 correlations had a p value less than 1.0×10^{-30} .



PSQI_BedTime: During the past month, when have you usually gone to bed at night?

PSQI_Min2Asleep: During the past month, how long has it usually taken you to fall asleep each night.

PSQI_GetUpTime: During the past month, when have you usually gotten up in the morning?

PSQI_Latency30Min: During the past month, how often have you had trouble sleeping because you... (a) Cannot get to sleep within 30 minutes; 0=Not during the past month, 1=Less than once a week, 2=Once or twice a week, 3=3 or more times a week.

PSQI_WakeUp: During the past month, how often have you had trouble sleeping because you... (b) Wake up in the middle of the night or early morning; 0=Not during the past month, 1=Less than once a week, 2=Once or twice a week, 3=3 or more times a week.

PSQI_Bathroom: During the past month, how often have you had trouble sleeping because you... (c) Have to get up to use the bathroom; 0=Not during the past month, 1=Less than once a week, 2=Once or twice a week, 3=3 or more times a week.

PSQI_Breathe: During the past month, how often have you had trouble sleeping because you... (d) Cannot breathe comfortably; 0=Not during the past month, 1=Less than once a week, 2=Once or twice a week, 3=3 or more times a week.

PSQI_Snore: During the past month, how often have you had trouble sleeping because you... (e) Cough or snore loudly; 0=Not during the past month, 1=Less than once a week, 2=Once or twice a week, 3=3 or more times a week.

PSQI_TooCold: During the past month, how often have you had trouble sleeping because you... (f) Feel too cold; 0=Not during the past month, 1=Less than once a week, 2=Once or twice a week, 3=3 or more times a week.

PSQI_TooHot: During the past month, how often have you had trouble sleeping because you... (g) Feel too hot; 0=Not during the past month, 1=Less than once a week, 2=Once or twice a week, 3=3 or more times a week.

PSQI_BadDream: During the past month, how often have you had trouble sleeping because you... (h) Had bad dreams; 0=Not during the past month, 1=Less than once a week, 2=Once or twice a week, 3=3 or more times a week.

PSQI_Pain: During the past month, how often have you had trouble sleeping because you... (i) Have pain; 0=Not during the past month, 1=Less than once a week, 2=Once or twice a week, 3=3 or more times a week.

PSQI_Other: During the past month, how often have you had trouble sleeping because of... (j) Other reason(s), as described in 5j. pt2 0=Not during the past month, 1=Less than once a week, 2=Once or twice a week, 3=3 or more times a week.

PSQI_Quality: During the past month, how would you rate your sleep quality overall?

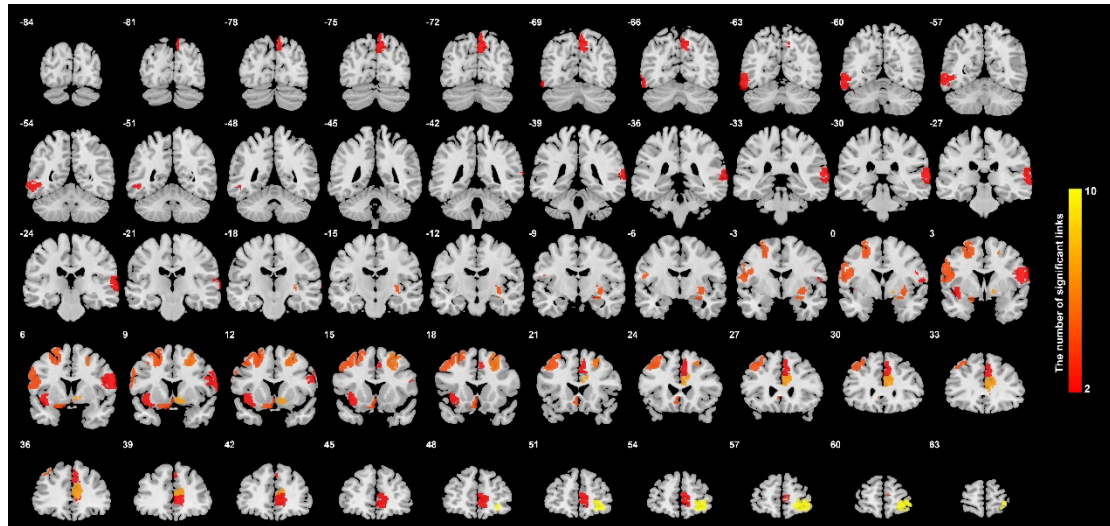
PSQI_SleepMeds: During the past month, how often have you taken medicine (prescribed or \"over the counter\") to help you sleep?

PSQI_DayStayAwake: During the past month, how often have you had trouble staying awake while driving, eating meals, or engaging in social activity?

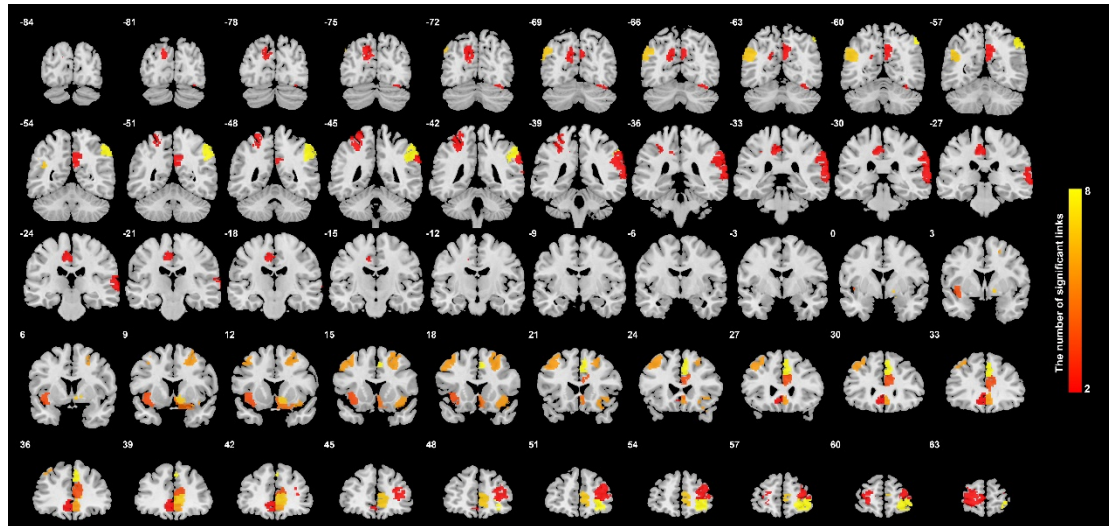
PSQI_DayEnthusiasm: During the past month, how much of a problem has it been for you to keep up enough enthusiasm to get things done?

PSQI_Comp1-7: the PSQI components.

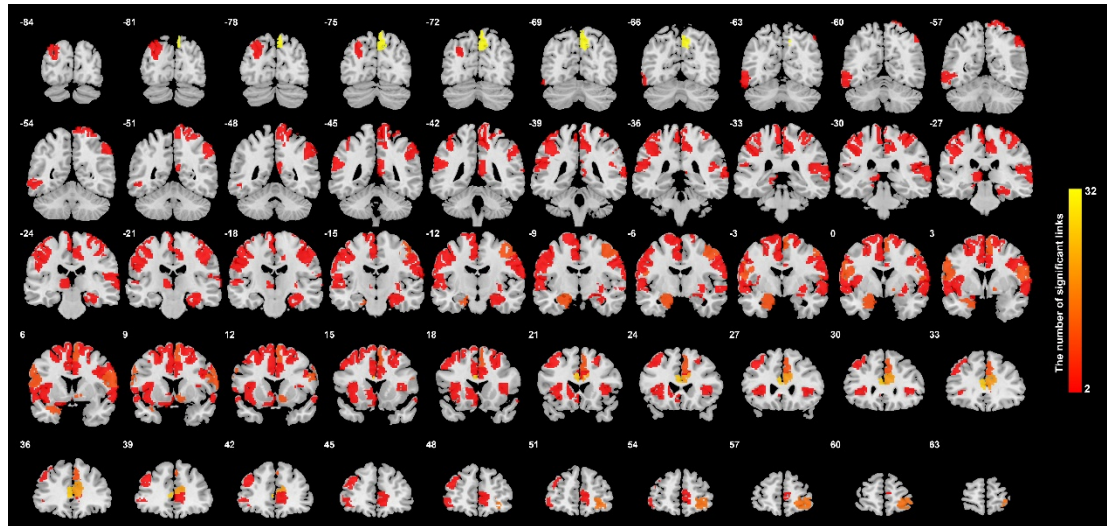
eFigure 2. Brain areas with functional connectivities related to both the sleep quality (PSQI) and the ASR DSM Depressive Problems scores from the HCP analysis. The color reflects the number of correlated links in each of the 250 areas in the atlas by Shen et al¹⁰. All of the links are positively correlated with the Depressive Problems score, and details are shown in Table S4. There were 39 such links (shown in Table S4, significant with NBS correction, $p < 0.05$).



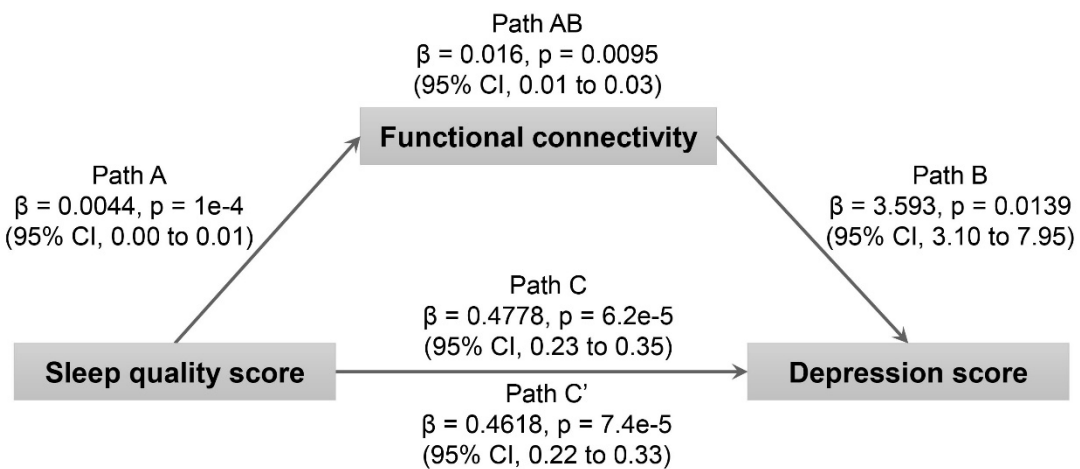
eFigure 3. Brain areas with functional connectivities related to the ASR DSM Depressive Problems scores from the HCP analysis. The significance value for the links to be included is $p < 0.005$ uncorrected. The color reflects the number of correlated links in each of the 250 areas in the atlas by Shen et al.¹⁰. Most of the links are positively correlated with the depressive problems score, and details are shown in Table S2.



eFigure 4. The Shen atlas areas with functional connectivities related to sleep quality. There were 162 such links significant with NBS correction, $p < 0.05$. All of the links are positively correlated with the sleep quality index (PSQI). The data here correspond to those in Fig. 1A. The amygdala is not included as a separate area in the Shen atlas, but does have FC related to sleep quality as shown here.



eFigure 5. Mediation analysis: the mediation implemented by functional connectivity from poor sleep quality (PSQI score) on the depressive problems score is significant (3.4% of the total effect size, $\beta=0.016$, $p=0.0095$). This provides evidence that the 39 functional connectivity links described in the paper may underlie the relation between sleep and depressive problems. Path A: the effect of sleep quality on the mediator (functional connectivity); Path B: the effect of the mediator (functional connectivity) on the outcome (depressive problems); Path C: the total effect of the sleep quality on the outcome (depressive problems); Path C': the direct effect of the sleep quality on the outcome (depressive problems) controlling for the mediator (functional connectivity). The beta values show the regression coefficient¹⁹ of the effect of the independent variable (the sleep quality score) on the dependent variable (the depressive problems score). It should be noted that the absolute values of beta cannot be compared with those in Fig. 2D since they are from a different regression model.



eTable 1. The anatomical regions defined in each hemisphere using the Shen atlas ¹⁰, with appropriate names provided for each Shen atlas region by finding the corresponding part in the AAL2 atlas ¹⁷.

No .	Region name	Anatomical description	No .	Region name	Anatomical description
1	OFCpost_R	Posterior orbitofrontal gyrus	126	Frontal_Mid_2_R	Middle frontal gyrus
2	OFCpost_L	Posterior orbitofrontal gyrus	127	Frontal_Sup_Media1_R	Superior frontal gyrus, medial
3	OFCant_R	Anterior orbitofrontal gyrus	128	Cuneus_R	Cuneus
4	OFCant_L	Anterior orbitofrontal gyrus	129	ParaHippocampal_R	Parahippocampal gyrus
5	OFCmed_R	Medial orbitofrontal gyrus	130	Cingulate_Post_R	Posterior cingulate gyrus
6	OFCmed_L	Medial orbitofrontal gyrus	131	Lingual_R	Lingual gyrus
7	Rectus_R	Gyrus rectus	132	Frontal_Mid_2_R	Middle frontal gyrus
8	Rectus_L	Gyrus rectus	133	Cingulate_Mid_R	Middle cingulate & paracingulate gyri
9	Olfactory_R	Olfactory cortex	134	Precentral_R	Precentral gyrus
10	Olfactory_L	Olfactory cortex	135	Frontal_Mid_2_L	Middle frontal gyrus
11	OFClat_R	Lateral orbitofrontal gyrus	136	Frontal_Inf_Tri_L	Inferior frontal gyrus, triangular part
12	OFClat_L	Lateral orbitofrontal gyrus	137	Frontal_Inf_Oper_L	Inferior frontal gyrus, opercular part
13	Frontal_Inf_Orb_2_R	Inferior Frontal Gyrus, orbital part	138	Precuneus_L	Precuneus
14	Frontal_Inf_Orb_2_L	Inferior Frontal Gyrus, orbital part	139	Temporal_Inf_L	Inferior temporal gyrus
15	Precentral_R	Precentral gyrus	140	Postcentral_L	Postcentral gyrus
16	Frontal_Sup_2_R	Superior frontal gyrus, dorsolateral	141	Putamen_L	Lenticular nucleus, Putamen
17	Frontal_Med_Orb_R	Superior frontal gyrus, medial orbital (or ventromedial prefrontal cortex)	142	Caudate_L	Caudate nucleus
18	Postcentral_R	Postcentral gyrus	143	Cingulate_Mid_L	Middle cingulate & paracingulate gyri
19	SupraMarginal_R	Supramarginal gyrus	144	Occipital_Mid_L	Middle occipital gyrus
20	OFClat2	Lateral orbitofrontal cortex	145	Postcentral_L	Postcentral gyrus
21	Precentral_R	Precentral gyrus	146	Thalamus_L	Thalamus
22	Postcentral_R	Postcentral gyrus	147	Calcarine_L	Calcarine fissure and surrounding cortex
23	Frontal_Mid_2_R	Middle frontal gyrus	148	Postcentral_L	Postcentral gyrus
24	Temporal_Inf_R	Inferior temporal gyrus	149	Parietal_Inf_L	Inferior parietal gyrus, excluding

© 2018 American Medical Association. All rights reserved.

					supramarginal and angular gyri
25	Thalamus_R	Thalamus	15 0	Cingulate_Ant_L	Anterior cingulate & paracingulate gyri
26	Lingual_R	Lingual gyrus	15 1	Insula_L	Insula
27	Calcarine_R	Calcarine fissure and surrounding cortex	15 2	Frontal_Mid_2_L	Middle frontal gyrus
28	Heschl_R	Heschl's gyrus	15 3	Calcarine_L	Calcarine fissure and surrounding cortex
29	Precuneus_R	Precuneus	15 4	Parietal_Inf_L	Inferior parietal gyrus, excluding supramarginal and angular gyri
30	SupraMarginal_R	Supramarginal gyrus	15 5	Thalamus_L	Thalamus
31	Temporal_Sup_R	Superior temporal gyrus	15 6	Lingual_L	Lingual gyrus
32	Temporal_Inf_R	Inferior temporal gyrus	15 7	Insula_L	Insula
33	Frontal_Inf_Tri_R	Inferior frontal gyrus, triangular part	15 8	Precuneus_L	Precuneus
34	Precuneus_R	Precuneus	15 9	Supp_Motor_Area_L	Supplementary motor area
35	Temporal_Mid_R	Middle temporal gyrus	16 0	Cingulate_Mid_L	Middle cingulate & paracingulate gyri
36	Angular_R	Angular gyrus	16 1	Cingulate_Mid_L	Middle cingulate & paracingulate gyri
37	Caudate_R	Caudate nucleus	16 2	Precentral_L	Precentral gyrus
38	Temporal_Pole_Mid_R	Temporal pole: middle temporal gyrus	16 3	Fusiform_L	Fusiform gyrus
39	Cingulate_Mid_R	Middle cingulate & paracingulate gyri	16 4	Frontal_Mid_2_L	Middle frontal gyrus
40	Postcentral_R	Postcentral gyrus	16 5	Cingulate_Ant_L	Anterior cingulate & paracingulate gyri
41	Parietal_Sup_R	Superior parietal gyrus	16 6	Temporal_Pole_Mid_L	Temporal pole: middle temporal gyrus
42	Postcentral_R	Postcentral gyrus	16 7	Cingulate_Ant_L	Anterior cingulate & paracingulate gyri
43	Temporal_Mid_R	Middle temporal gyrus	16 8	Temporal_Sup_L	Superior temporal gyrus
44	Postcentral_R	Postcentral gyrus	16 9	Calcarine_L	Calcarine fissure and surrounding cortex
45	Temporal_Inf_R	Inferior temporal gyrus	17 0	Occipital_Mid_L	Middle occipital gyrus
46	Cuneus_R	Cuneus	17 1	Precuneus_L	Precuneus
47	Frontal_Sup_Medial_R	Superior frontal gyrus, medial	17 2	Supp_Motor_Area_L	Supplementary motor area
48	Occipital_Mid_R	Middle occipital gyrus	17 3	Temporal_Pole_Sup_L	Temporal pole: superior temporal gyrus

© 2018 American Medical Association. All rights reserved.

49	Occipital_Sup_R	Superior occipital gyrus	17 4	Cuneus_L	Cuneus
50	Precuneus_R	Precuneus	17 5	Hippocampus_L	Hippocampus
51	ParaHippocampal_R	Parahippocampal gyrus	17 6	Angular_L	Angular gyrus
52	Insula_R	Insula	17 7	Frontal_Mid_Orb_R (or OFClat)	Lateral orbital gyrus
53	Temporal_Sup_R	Superior temporal gyrus	17 8	Angular_L	Angular gyrus
54	Precuneus_R	Precuneus	17 9	SupraMarginal_L	Supramarginal gyrus
55	Frontal_Sup_Media_L_R	Superior frontal gyrus, medial	18 0	Precentral_L	Precentral gyrus
56	Cingulate_Post_R	Posterior cingulate cortex (retrosplenial)	18 1	Temporal_Inf_L	Inferior temporal gyrus
57	Calcarine_R	Calcarine fissure and surrounding cortex	18 2	Hippocampus_L	Hippocampus
58	Postcentral_R	Postcentral gyrus	18 3	Frontal_Sup_2_L	Superior frontal gyrus, dorsolateral
59	Temporal_Mid_R	Middle temporal gyrus	18 4	Temporal_Inf_L	Inferior temporal gyrus
60	Caudate_R	Caudate nucleus	18 5	Frontal_Sup_2_L	Superior frontal gyrus, dorsolateral
61	Calcarine_R	Calcarine fissure and surrounding cortex	18 6	Cingulate_Post_L	Posterior cingulate gyrus
62	Cingulate_Ant_R	Anterior cingulate & paracingulate gyri	18 7	Lingual_L	Lingual gyrus
63	Cingulate_Mid_R	Middle cingulate & paracingulate gyri	18 8	Precentral_L	Precentral gyrus
64	Temporal_Sup_R	Superior temporal gyrus	18 9	Insula_L	Insula
65	Postcentral_R	Postcentral gyrus	19 0	Lingual_L	Lingual gyrus
66	Hippocampus_R	Hippocampus	19 1	Temporal_Mid_L	Middle temporal gyrus
67	Supp_Motor_Area_R	Supplementary motor area	19 2	Temporal_Mid_L	Middle temporal gyrus
68	Parietal_Sup_R	Superior parietal gyrus	19 3	Fusiform_L	Fusiform gyrus
69	Temporal_Mid_R	Middle temporal gyrus	19 4	Occipital_Mid_L	Middle occipital gyrus
70	Frontal_Mid_2_R	Middle frontal gyrus	19 5	Frontal_Inf_Tri_L	Inferior frontal gyrus, triangular part
71	Frontal_Sup_2_R	Superior frontal gyrus, dorsolateral	19 6	Insula_L	Insula
72	Frontal_Med_Orb_R	Superior frontal gyrus, medial orbital (or ventromedial prefrontal cortex)	19 7	Fusiform_L	Fusiform gyrus
73	Frontal_Mid_2_R	Middle frontal gyrus	19 8	Temporal_Sup_L	Superior temporal gyrus
74	Cingulate_Ant_R	Anterior cingulate & paracingulate gyri	19 9	Parietal_Inf_L	Inferior parietal gyrus, excluding supramarginal and angular gyri
75	Temporal_Pole_Mid_R	Temporal pole: middle temporal gyrus	20 0	Occipital_Mid_L	Middle occipital gyrus

© 2018 American Medical Association. All rights reserved.

76	Cingulate_Mid_R	Middle cingulate & paracingulate gyri	20 1	Cuneus_L	Cuneus
77	Frontal_Mid_2_R	Middle frontal gyrus	20 2	Precuneus_L	Precuneus
78	Fusiform_R	Fusiform gyrus	20 3	Frontal_Sup_Media 1_L	Superior frontal gyrus, medial
79	Temporal_Sup_R	Superior temporal gyrus	20 4	Frontal_Mid_2_L	Middle frontal gyrus
80	Hippocampus_R	Hippocampus	20 5	Lingual_L	Lingual gyrus
81	Temporal_Pole_Sup_R	Temporal pole: superior temporal gyrus	20 6	Frontal_Sup_2_L	Superior frontal gyrus, dorsolateral
82	Parietal_Sup_R	Superior parietal gyrus	20 7	Temporal_Mid_L	Middle temporal gyrus
83	Cingulate_Ant_R	Anterior cingulate & paracingulate gyri	20 8	Cingulate_Mid_L	Middle cingulate & paracingulate gyri
84	Insula_R	Insula	20 9	Parietal_Sup_L	Superior parietal gyrus
85	Temporal_Sup_R	Superior temporal gyrus	21 0	Hippocampus_L	Hippocampus
86	Cuneus_R	Cuneus	21 1	Temporal_Mid_L	Middle temporal gyrus
87	Frontal_Sup_2_R	Superior frontal gyrus, dorsolateral	21 2	Fusiform_L	Fusiform gyrus
88	Fusiform_R	Fusiform gyrus	21 3	Lingual_L	Lingual gyrus
89	Frontal_Mid_2_R	Middle frontal gyrus	21 4	Temporal_Sup_L	Superior temporal gyrus
90	Temporal_Mid_R	Middle temporal gyrus	21 5	Temporal_Inf_L	Inferior temporal gyrus
91	Temporal_Inf_R	Inferior temporal gyrus	21 6	Parietal_Sup_L	Superior parietal gyrus
92	Insula_R	Insula	21 7	SupraMarginal_L	Supramarginal gyrus
93	Cingulate_Mid_R	Middle cingulate & paracingulate gyri	21 8	Precentral_L	Precentral gyrus
94	Insula_R	Insula	21 9	Temporal_Inf_L	Inferior temporal gyrus
95	Parietal_Inf_R	Inferior parietal gyrus, excluding supramarginal and angular gyri	22 0	Temporal_Pole_Sup_L	Temporal pole: superior temporal gyrus
96	Temporal_Mid_R	Middle temporal gyrus	22 1	SupraMarginal_L	Supramarginal gyrus
97	Lingual_R	Lingual gyrus	22 2	Insula_L	Insula
98	Fusiform_R	Fusiform gyrus	22 3	Occipital_Inf_L	Inferior occipital gyrus
99	Putamen_R	Lenticular nucleus, Putamen	22 4	Frontal_Sup_Media 1_L	Superior frontal gyrus, medial
100	Insula_R	Insula	22 5	Precuneus_L	Precuneus
101	Parietal_Inf_R	Inferior parietal gyrus, excluding supramarginal and angular gyri	22 6	Occipital_Mid_L	Middle occipital gyrus
102	Frontal_Sup_2_R	Superior frontal gyrus, dorsolateral	22 7	Frontal_Mid_2_L	Middle frontal gyrus

© 2018 American Medical Association. All rights reserved.

103	Occipital_Inf_R	Inferior occipital gyrus	228	Paracentral_Lobule_L	Paracentral lobule
104	Frontal_Inf_Tri_R	Inferior frontal gyrus, triangular part	229	Postcentral_L	Postcentral gyrus
105	Supp_Motor_Area_R	Supplementary motor area	230	Precuneus_L	Precuneus
106	Occipital_Sup_R	Superior occipital gyrus	231	Occipital_Inf_L	Inferior occipital gyrus
107	Frontal_Inf_Tri_R	Inferior frontal gyrus, triangular part	232	Cingulate_Mid_L	Middle cingulate & paracingulate gyri
108	Fusiform_R	Fusiform gyrus	233	Frontal_Mid_2_L	Middle frontal gyrus
109	Fusiform_R	Fusiform gyrus	234	Thalamus_L	Thalamus
110	Frontal_Inf_Oper_R	Inferior frontal gyrus, opercular part	235	Postcentral_L	Postcentral gyrus
111	Fusiform_R	Fusiform gyrus	236	Caudate_L	Caudate nucleus
112	Fusiform_R	Fusiform gyrus	237	Cingulate_Mid_L	Middle cingulate & paracingulate gyri
113	Caudate_R	Caudate nucleus	238	Temporal_Pole_Mid_L	Temporal pole: middle temporal gyrus
114	Precentral_R	Precentral gyrus	239	Hippocampus_L	Hippocampus
115	Lingual_R	Lingual gyrus	240	Frontal_Sup_Medial_L	Superior frontal gyrus, medial
116	Thalamus_R	Thalamus	241	Temporal_Sup_L	Superior temporal gyrus
117	Frontal_Med_Orb_R	Superior frontal gyrus, medial orbital (or ventromedial prefrontal cortex)	242	Insula_L	Insula
118	Occipital_Mid_R	Middle occipital gyrus	243	Calcarine_L	Calcarine fissure and surrounding cortex
119	Occipital_Mid_R	Middle occipital gyrus	244	Cingulate_Ant_L	Anterior cingulate & paracingulate gyri
120	Temporal_Mid_R	Middle temporal gyrus	245	Caudate_L	Caudate nucleus
121	Temporal_Pole_Mid_R	Temporal pole: middle temporal gyrus	246	Frontal_Med_Orb_L	Superior frontal gyrus, medial orbital (or ventromedial prefrontal cortex)
122	Frontal_Inf_Oper_R	Inferior frontal gyrus, opercular part	247	Occipital_Mid_L	Middle occipital gyrus
123	Parietal_Inf_R	Inferior parietal gyrus, excluding supramarginal and angular gyri	248	Frontal_Inf_Tri_L	Inferior frontal gyrus, triangular part
124	Calcarine_R	Calcarine fissure and surrounding cortex	249	Supp_Motor_Area_L	Supplementary motor area
125	Putamen_R	Lenticular nucleus, Putamen	250	Postcentral_L	Postcentral gyrus

Note: _L indicates left hemisphere; _R indicates right hemisphere;

The AAL2 names provided were obtained by mapping the MNI coordinates of each Shen atlas area to the corresponding AAL2 atlas area¹⁷.

© 2018 American Medical Association. All rights reserved.

eTable 2. Functional connectivities related to the ASR DSM Depressive Problems scores from the HCP analysis using 1017 participants. The significance value for the links to be included is $p < 0.005$ uncorrected. Each link is between two areas defined in the atlas by Shen et al¹⁰. A link positively correlated with the Depressive Problems score indicates that the functional connectivity of that link is positively correlated with the Depressive Problems score. The brain area names used are those for the corresponding AAL2 area as shown in Table S1. A Shen area in BA 12 has been included in OFClat. The functional connectivities of the lateral orbitofrontal cortex areas (OFClat, OFClat2, and Frontal_Inf_Orb2) were especially related to depression, in that removing the 92 participants who had ever been diagnosed with depression (leaving the column headed 'Participants who had never been diagnosed with depression') decreased the absolute value of the correlations by 0.036, whereas this removal decreased the correlation for the other functional connectivity links by only 0.023 ($p = 0.053$)

Functional connectivity		All participants		Participants who had never been diagnosed with depression		Functional connectivity		All participants		Participants who had never been diagnosed with depression	
		r value	p value	r value	p value			r value	p value	r value	p value
Cingulate_Ant_R	Frontal_Mid_2_L	0.125	0.0001	0.084	0.013	Frontal_Mid_2_R	Cingulate_Ant_R	0.107	0.0027	0.115	0.001
Insula_R	Cingulate_Ant_R	0.122	0.0002	0.087	0.0097	Frontal_Mid_2_R	Frontal_Med_Orb_R	0.101	0.0027	0.068	0.0474
OFClat2	Insula_L	0.120	0.0003	0.080	0.0165	Frontal_Mid_2_R	Insula_L	0.101	0.0027	0.083	0.0115
Cingulate_Ant_R	Frontal_Mid_2_L	0.124	0.0003	0.085	0.0121	Cingulate_Mid_R	Frontal_Mid_2_L	0.093	0.0027	0.062	0.0719
Cuneus_L	Frontal_Sup_2_L	-0.115	0.0004	-0.109	0.0016	OFClat2	Cingulate_Ant_R	0.106	0.0029	0.061	0.0767
Rectus_R	Cuneus_L	-0.113	0.0005	-0.095	0.0046	Parietal_Inf_R	Temporal_Pole_Sup_L	0.099	0.0029	0.059	0.0867
Frontal_Mid_2_R	Angular_L	0.104	0.0006	0.062	0.0702	Caudate_R	Frontal_Inf_Tri_L	0.097	0.0033	0.077	0.0226
Cingulate_Mid_R	Angular_L	0.111	0.0006	0.065	0.0535	Cingulate_Ant_R	Angular_L	0.097	0.0033	0.042	0.1991
Frontal_Mid_2_R	Frontal_Med_Orb_R	0.112	0.0009	0.101	0.0021	Caudate_R	Frontal_Mid_2_L	0.095	0.0034	0.096	0.0035
SupraMarginal_R	Temporal_Sup_R	0.107	0.001	0.081	0.015	Precuneus_R	Cingulate_Mid_R	0.095	0.0035	0.081	0.017

					4						6
Frontal_Mid_2_R	Angular_L	0.108	0.001	0.104	0.0021	Cingulate_Ant_R	Precentral_L	0.099	0.0035	0.047	0.1723
Frontal_Inf_Orb_2_R	Cingulate_Ant_R	0.111	0.0011	0.069	0.0436	Fusiform_R	Cuneus_L	-0.093	0.0035	-0.062	0.0612
Cingulate_Ant_R	Cingulate_Mid_R	0.100	0.0012	0.074	0.0332	Parietal_Inf_R	Cingulate_Mid_L	0.102	0.0035	0.111	0.0018
Frontal_Med_Orb_R	Cingulate_Mid_R	0.107	0.0013	0.070	0.0403	Frontal_Mid_2_R	Cingulate_Ant_L	0.096	0.0036	0.100	0.0028
Temporal_Inf_R	Postcentral_L	-0.103	0.0013	-0.099	0.0033	OFClat2	Insula_L	0.099	0.0037	0.062	0.0659
Cingulate_Mid_R	Cingulate_Ant_L	0.103	0.0015	0.084	0.0146	Insula_R	Frontal_Med_Orb_R	0.097	0.0038	0.072	0.0342
Parietal_Inf_R	Hippocampus_L	0.108	0.0016	0.079	0.0194	Insula_R	Angular_L	0.099	0.0038	0.065	0.0531
Parietal_Inf_R	Fusiform_R	0.107	0.0018	0.074	0.0296	OFClat2	SupraMarginal_R	0.093	0.0039	0.054	0.1066
Olfactory_R	Cingulate_Mid_R	0.098	0.002	0.037	0.2884	Cingulate_Mid_R	Caudate_R	0.092	0.0039	0.084	0.0108
OFClat_L	Frontal_Sup_2_L	0.098	0.0021	0.095	0.0055	Olfactory_R	Caudate_L	0.091	0.004	0.040	0.243
OFClat2	Frontal_Mid_2_R	0.098	0.0022	0.071	0.0366	Olfactory_R	Frontal_Mid_2_R	0.098	0.0041	0.068	0.0407
Angular_L	Frontal_Sup_Medial_L	-0.096	0.0023	-0.055	0.0984	Parietal_Inf_R	Temporal_Mid_R	0.094	0.0042	0.116	0.0005
Precentral_R	OFClat2	0.100	0.0024	0.050	0.1368	Postcentral_L	Temporal_Inf_L	-0.092	0.0044	-0.097	0.0042
OFClat2	Insula_R	0.096	0.0024	0.067	0.0451	OFCpost_L	Frontal_Sup_Medial_R	0.091	0.0045	0.072	0.0376
Olfactory_R	Parietal_Inf_R	0.103	0.0024	0.036	0.2849	Insula_R	Frontal_Mid_2_L	0.091	0.0045	0.081	0.0144
Caudate_R	Insula_L	0.099	0.0024	0.087	0.01	Precentral_L	Cingulate_Mid_L	0.092	0.0045	0.057	0.0999
Cingulate_Mid_R	Precuneus_L	0.097	0.0024	0.082	0.0155	Temporal_Sup_R	Parietal_Inf_R	0.091	0.0046	0.075	0.0258

© 2018 American Medical Association. All rights reserved.

Precuneus_R	Insula_R	0.101	0.0025	0.081	0.018 1	Caudate_R	Insula_L	0.091	0.0046	0.077	0.027 3
Cuneus_R	Fusiform_R	-0.097	0.0025	-0.06 5	0.050 8	Frontal_Med_Orb_ R	Cingulate_Ant_L	0.095	0.0049	0.059	0.081 6
OFClat2	SupraMarginal_L	0.095	0.0025	0.048	0.146 9	Parietal_Inf_R	Lingual_L	0.095	0.0049	0.097	0.008 3
Caudate_R	Cingulate_Mid_L	0.095	0.0025	0.095	0.005 2						

eTable 3. Functional connectivities correlated with the ASR DSM Depressive Problems scores from the HCP analysis based on the 92 participants who had at some time been diagnosed with depression. The 58 links with a p-value < 0.001 uncorrected are shown. As shown in the Table the anterior cingulate cortex (Cingulate_Ant) had 8 links significant at this level, and the lateral orbitofrontal cortex (OFClat_2/Frontal_Inf_Orb) had 8 links. The other brain areas with more than 3 significant links included Angular (12 links), ParaHippocampal (7), Frontal_Mid_2 (12), Temporal (18), OFCant (3) and Cingulate_Mid (9).

Functional connectivity		p value	r value	Functional connectivity		p value	r value
Parietal_Inf_R	ParaHippocampal_R	0.464	<0.0001	Temporal_Pole_Sup_R	Frontal_Sup_Medial_L	0.353	0.0006
Cingulate_Ant_R	Supp_Motor_Area_L	0.446	<0.0001	OFClat2	Cingulate_Mid_L	0.385	0.0006
OFCant_R	Temporal_Inf_L	0.476	<0.0001	Frontal_Mid_2_L	Cingulate_Mid_L	0.347	0.0006
Precuneus_R	Temporal_Inf_L	0.383	<0.0001	Occipital_Mid_R	Fusiform_L	0.351	0.0006
OFClat2	Frontal_Mid_2_L	0.410	<0.0001	Angular_L	Postcentral_L	0.383	0.0006
ParaHippocampal_R	Angular_L	0.370	0.0002	Temporal_Inf_L	Frontal_Mid_2_L	0.354	0.0006
Parietal_Inf_R	Temporal_Pole_Sup_L	0.444	0.0002	OFClat2	Cingulate_Mid_R	0.368	0.0007
Angular_L	Temporal_Pole_Sup_L	0.422	0.0002	Parietal_Inf_R	Fusiform_R	0.375	0.0007
Postcentral_R	Cingulate_Ant_R	0.368	0.0003	Olfactory_R	Frontal_Mid_2_R	0.345	0.0007
Frontal_Mid_2_R	ParaHippocampal_R	0.399	0.0003	Postcentral_R	Angular_L	0.362	0.0007
Temporal_Pole_Sup_R	Precentral_L	0.364	0.0003	Fusiform_R	Angular_L	0.350	0.0007
Angular_R	Temporal_Sup_L	0.360	0.0003	Cingulate_Ant_R	Temporal_Inf_L	0.365	0.0007
OFCant_R	Temporal_Inf_L	0.366	0.0003	Cingulate_Mid_R	Temporal_Inf_L	0.337	0.0007
Frontal_Mid_2_R	Frontal_Mid_2_L	0.388	0.0003	OFClat2	Precuneus_L	0.430	0.0007
OFClat2	Cingulate_Mid_R	0.402	0.0004	Occipital_Mid_R	Calcarine_L	0.367	0.0008
Temporal_Pole_Sup_R	Cingulate_Ant_R	0.338	0.0004	Cingulate_Ant_R	Frontal_Mid_2_L	0.321	0.0008
Angular_R	Frontal_Mid_2_L	0.420	0.0004	Temporal_Mid_R	Cingulate_Mid_L	0.336	0.0008
Precuneus_R	Temporal_Inf_L	0.381	0.0004	Cingulate_Ant_R	Occipital_Mid_L	0.329	0.0008
Occipital_Sup_R	Occipital_Mid_L	0.347	0.0004	Olfactory_R	Frontal_Mid_2_R	0.369	0.0009
ParaHippocampal_R	Parietal_Inf_L	0.395	0.0004	Temporal_Mid_R	ParaHippocampal_R	0.359	0.0009
Cuneus_R	Parietal_Sup_L	0.394	0.0004	Frontal_Mid_2_R	ParaHippocampal_R	0.360	0.0009
Temporal_Mid_R	Postcentral_L	0.351	0.0004	Cingulate_Ant_R	Frontal_Inf_Oper_L	0.373	0.0009
Frontal_Inf_Orb_2_L	Cingulate_Ant_R	0.393	0.0005	Postcentral_R	Angular_L	0.382	0.0009
Parietal_Inf_R	Angular_L	0.386	0.0005	Angular_R	SupraMarginal_L	0.374	0.0009
OFClat2	SupraMarginal_L	0.377	0.0005	OFCant_R	Temporal_Mid_L	0.363	0.0009
Angular_R	Cingulate_Mid_L	0.428	0.0005	Frontal_Mid_2_R	Temporal_Mid_L	0.363	0.0009
Angular_R	Frontal_Mid_2_L	0.378	0.0005	Parietal_Sup_R	Occipital_Mid_L	0.336	0.0009
ParaHippocampal_R	Cingulate_Mid_R	0.350	0.0006	OFClat2	Insula_L	0.348	0.0009

eTable 4. The results of the mediation analysis performed for the 39 individual links that were correlated with sleep quality and the Depressive Problems score. The analysis is analogous to that shown in Fig. 2D, but here is for individual links, instead of for the mean value of the functional connectivity of these 39 links. The paths correspond to those shown in Fig. 2D. All 39 links were found to underlie the relation between sleep quality and the Depressive Problems score in this analysis. A positive beta for path A indicates a positive correlation between the functional connectivity and the Depressive Problems score.

Functional connectivity		path A		path B		path C'		path C		path AB	
		Beta	p value	beta	p value	beta	p value	beta	p value	beta	p value
Cingulate_Ant_R	Frontal_Mid_2_L	0.00511	0.00018	1.31786	0.02379	0.28144	0.00013	0.28817	0.00012	0.00673	0.01452
OFClat2	Insula_L	0.00400	0.00017	1.71605	0.01497	0.28130	0.00013	0.28817	0.00011	0.00687	0.00912
Cingulate_Ant_R	Frontal_Mid_2_L	0.00467	0.00019	1.24311	0.02753	0.28236	0.00012	0.28817	0.00010	0.00581	0.01925
Precentral_R	OFClat2	0.00364	0.00228	1.55282	0.01186	0.28251	0.00012	0.28817	0.00010	0.00566	0.00666
Caudate_R	Frontal_Inf_Tri_L	0.00139	0.00212	4.32195	0.00333	0.28218	0.00009	0.28817	0.00009	0.00599	0.00281
OFClat2	Cingulate_Mid_R	0.00359	0.00176	1.45532	0.01246	0.28294	0.00013	0.28817	0.00010	0.00523	0.00666
OFClat2	Insula_L	0.00287	0.00672	1.77966	0.00890	0.28307	0.00012	0.28817	0.00011	0.00510	0.00745
OFClat2	Frontal_Mid_2_L	0.00443	0.00700	1.30637	0.00435	0.28239	0.00013	0.28817	0.00012	0.00578	0.00562
OFClat2	Insula_L	0.00270	0.00361	2.12378	0.00247	0.28244	0.00011	0.28817	0.00010	0.00573	0.00288
OFClat2	Precentral_R	0.00368	0.00998	1.53636	0.00295	0.28251	0.00010	0.28817	0.00009	0.00566	0.00603
OFClat2	Cingulate_Mid_L	0.00334	0.00388	1.60279	0.00730	0.28282	0.00012	0.28817	0.00010	0.00535	0.00457
Caudate_R	Precentral_L	0.00104	0.01472	4.65151	0.00573	0.28334	0.00009	0.28817	0.00009	0.00483	0.01050
Cingulate_Ant_R	Frontal_Mid_2_L	0.00275	0.00653	1.96448	0.00359	0.28276	0.00012	0.28817	0.00011	0.00541	0.00513
Cingulate_Ant_L	Frontal_Mid_2_L	0.00247	0.00331	1.90866	0.00451	0.28346	0.00011	0.28817	0.00010	0.00471	0.00386
Caudate_R	Frontal_Sup_2_L	0.00115	0.00562	5.43865	0.00118	0.28191	0.00009	0.28817	0.00009	0.00626	0.00376
OFClat2	Precentral_L	0.00266	0.01140	2.50328	0.00011	0.28152	0.00010	0.28817	0.00008	0.00665	0.00525
Frontal_Mid_2_R	Precuneus_L	0.00393	0.00389	1.26098	0.00487	0.28322	0.00010	0.28817	0.00009	0.00495	0.00489
Cingulate_Mid_R	Frontal_Mid_Orb_R (orOFClat)	0.00326	0.01015	1.46925	0.00786	0.28338	0.00010	0.28817	0.00010	0.00479	0.00811
Frontal_Mid_2_R	Hippocampus_L	0.00227	0.00511	2.09409	0.01261	0.28342	0.00010	0.28817	0.00008	0.00475	0.00999
OFClat2	Temporal_Sup_L	0.00274	0.01427	2.05161	0.00141	0.28255	0.00009	0.28817	0.00009	0.00562	0.00841
Temporal_Sup_R	Cingulate_Ant_R	0.00265	0.01114	1.95903	0.00510	0.28297	0.00010	0.28817	0.00010	0.00520	0.00835
Caudate_R	Supp_Motor_Area_L	0.00103	0.02722	4.27949	0.00695	0.28376	0.00011	0.28817	0.00011	0.00441	0.01835
Cingulate_Ant_R	Occipital_Mid_L	0.00240	0.01055	2.21159	0.00182	0.28286	0.00012	0.28817	0.00010	0.00531	0.00607
Precuneus_R	Insula_L	0.00271	0.02087	1.91137	0.00239	0.28300	0.00012	0.28817	0.00010	0.00517	0.01223
Precentral_R	Caudate_R	0.00097	0.01668	5.33203	0.00193	0.28301	0.00010	0.28817	0.00011	0.00516	0.01063
Olfactory_L	Frontal_Sup_2_L	0.00145	0.02277	3.35740	0.00189	0.28330	0.00011	0.28817	0.00011	0.00487	0.01425

Temporal_Sup_R	Putamen_R	0.00213	0.03281	2.01796	0.00962	0.28387	0.00010	0.28817	0.00008	0.00430	0.02195
Olfactory_L	Hippocampus_R	0.00078	0.03200	5.43644	0.01144	0.28394	0.00012	0.28817	0.00012	0.00423	0.02378
Temporal_Sup_R	Cingulate_Mid_R	0.00314	0.02490	1.40705	0.01160	0.28374	0.00013	0.28817	0.00012	0.00442	0.01972
Frontal_Mid_2_R	Frontal_Sup_Medial_L	0.00325	0.01016	1.34193	0.00771	0.28380	0.00010	0.28817	0.00010	0.00437	0.00923
Cingulate_Ant_R	Temporal_Inf_L	0.00275	0.03044	1.60004	0.00818	0.28376	0.00009	0.28817	0.00008	0.00441	0.02067
Cingulate_Ant_R	Frontal_Sup_2_L	0.00249	0.01388	2.10435	0.00133	0.28294	0.00012	0.28817	0.00010	0.00523	0.00705
Precuneus_R	Insula_R	0.00315	0.01736	1.74555	0.00097	0.28267	0.00012	0.28817	0.00010	0.00550	0.00933
Olfactory_L	Frontal_Mid_2_R	0.00134	0.01566	3.89546	0.00157	0.28294	0.00010	0.28817	0.00010	0.00522	0.00959
Postcentral_R	Caudate_R	0.00102	0.06300	4.23258	0.00323	0.28383	0.00008	0.28817	0.00009	0.00434	0.03925
Putamen_R	Fusiform_R	0.00090	0.06561	4.52322	0.00760	0.28411	0.00011	0.28817	0.00009	0.00405	0.04275
Thalamus_L	Precentral_L	0.00158	0.06823	2.99203	0.00079	0.28345	0.00011	0.28817	0.00010	0.00472	0.03799
Cingulate_Ant_R	Temporal_Inf_L	0.00203	0.03308	2.20041	0.00203	0.28369	0.00011	0.28817	0.00010	0.00448	0.02032
Precentral_R	Putamen_R	0.00162	0.04949	2.67065	0.00273	0.28384	0.00011	0.28817	0.00010	0.00432	0.02913

eTable 5. The demographic characteristics of participants of the Biobank dataset.

Basic information on the participants						
Age (year)	Gender (Male / Female)	Diastolic blood pressure 1	Diastolic blood pressure 2	Qualifications (education)	BMI	Ever taken cannabis (no / yes)
62.30 ± 7.48 3,696	4695 / 5155	78.60 ± 10.27	78.52 ± 9.78	2.17 ± 1.47	26.65 ± 3.99	4784 / 1755
Smoking status (Never / Previous / Current)	Frequency of drinking alcohol	Amount of alcohol drunk on a typical drinking day	Mean framewise displacement	Volume of white matter	Volume of grey matter	Sleeplessness / insomnia (never / sometimes / usually)
1755 / 2917 / 360	2.42 ± 1.06	1.47 ± 0.99	0.182 ± 0.092	587987 ± 88192	650103 ± 88627	2259 / 4578 / 2937
Sleep duration						
7.150 ± 1.036						

Values are n or mean ± SD.

Sleep duration measure: 'If the time you spend sleeping varies a lot, give the average time for a 24 hour day in the last 4 weeks.'

Sleeplessness / insomnia: "Do you have trouble falling asleep at night or do you wake up in the middle of the night?"

Note: some participants chose 'prefer not to answer', so the number of participants of each terms may differ.

References

1. Glasser MF, Sotiropoulos SN, Wilson JA, et al. The minimal preprocessing pipelines for the Human Connectome Project. *Neuroimage*. 2013;80:105-124.
2. Navarro Schroder T, Haak KV, Zaragoza Jimenez NI, Beckmann CF, Doeller CF. Functional topography of the human entorhinal cortex. *Elife*. 2015;4.
3. Smith SM, Beckmann CF, Andersson J, et al. Resting-state fMRI in the Human Connectome Project. *Neuroimage*. 2013;80:144-168.
4. Salimi-Khorshidi G, Douaud G, Beckmann CF, Glasser MF, Griffanti L, Smith SM. Automatic denoising of functional MRI data: combining independent component analysis and hierarchical fusion of classifiers. *Neuroimage*. 2014;90:449-468.
5. Griffanti L, Salimi-Khorshidi G, Beckmann CF, et al. ICA-based artefact removal and accelerated fMRI acquisition for improved resting state network imaging. *Neuroimage*. 2014;95:232-247.
6. Colclough GL, Smith SM, Nichols TE, et al. The heritability of multi-modal connectivity in human brain activity. *Elife*. 2017;6.
7. Vidaurre D, Abeyesuriya R, Becker R, et al. Discovering dynamic brain networks from big data in rest and task. *Neuroimage*. 2017.
8. Smith SM, Nichols TE, Vidaurre D, et al. A positive-negative mode of population covariation links brain connectivity, demographics and behavior. *Nat Neurosci*. 2015;18(11):1565-1567.
9. Miller KL, Alfaro-Almagro F, Bangerter NK, et al. Multimodal population brain imaging in the UK Biobank prospective epidemiological study. *Nat Neurosci*. 2016;19(11):1523-1536.
10. Shen X, Tokoglu F, Papademetris X, Constable RT. Groupwise whole-brain parcellation from resting-state fMRI data for network node identification. *Neuroimage*. 2013;82:403-415.
11. Rosenberg MD, Finn ES, Scheinost D, et al. A neuromarker of sustained attention from whole-brain functional connectivity. *Nat Neurosci*. 2016;19(1):165-171.
12. Finn ES, Shen X, Scheinost D, et al. Functional connectome fingerprinting:

identifying individuals using patterns of brain connectivity. *Nat Neurosci*. 2015;18(11):1664-1671.

13. Zalesky A, Fornito A, Bullmore ET. Network-based statistic: identifying differences in brain networks. *Neuroimage*. 2010;53(4):1197-1207.

14. Zalesky A, Fornito A, Seal ML, et al. Disrupted axonal fiber connectivity in schizophrenia. *Biol Psychiatry*. 2011;69(1):80-89.

15. Zhang J, Wang J, Wu Q, et al. Disrupted brain connectivity networks in drug-naive, first-episode major depressive disorder. *Biol Psychiatry*. 2011;70(4):334-342.

16. Krienen FM, Yeo BT, Ge T, Buckner RL, Sherwood CC. Transcriptional profiles of supragranular-enriched genes associate with corticocortical network architecture in the human brain. *Proc Natl Acad Sci U S A*. 2016;113(4):E469-478.

17. Rolls ET, Joliot M, Tzourio-Mazoyer N. Implementation of a new parcellation of the orbitofrontal cortex in the automated anatomical labeling atlas. *Neuroimage*. 2015;122:1-5.

18. Dietch JR, Taylor DJ, Sethi K, Kelly K, Bramoweth AD, Roane BM. Psychometric Evaluation of the PSQI in U.S. College Students. *J Clin Sleep Med*. 2016;12(8):1121-1129.

19. Preacher KJ, Kelley K. Effect size measures for mediation models: quantitative strategies for communicating indirect effects. *Psychol Methods*. 2011;16(2):93-115.